

Article

# Understanding the Burial and Migration Characteristics of Deep Geothermal Water Using Hydrogen, Oxygen, and Inorganic Carbon Isotopes

Xinyi Wang <sup>1,2,3</sup>, Weifang Qiao <sup>1,4,\*</sup>, Jing Chen <sup>1</sup>, Xiaoman Liu <sup>1</sup> and Fang Yang <sup>5</sup>

<sup>1</sup> Institute of Resources & Environment, Henan Polytechnic University, Jiaozuo 454000, China; wangxy@hpu.edu.cn (X.W.); 18790202663@hpu.edu.cn (J.C.); liuxm@hpu.edu.cn (X.L.)

<sup>2</sup> Collaborative Innovation Center of Coalbed Methane and Shale Gas for Central Plains Economic Region, Jiaozuo 454000, China

<sup>3</sup> Institute of China PingMeiShenMa Group, Pingdingshan 467000, China

<sup>4</sup> School of Surveying and Land Information Engineering, Henan Polytechnic University, Jiaozuo 454000, China

<sup>5</sup> Office of Water Conservation in Kaifeng, Kaifeng 475002, China; yangfang@hpu.edu.cn

\* Correspondence: qiaoweifang@hpu.edu.cn; Tel.: +86-138-0391-3424

Received: 28 October 2017; Accepted: 19 December 2017; Published: 22 December 2017

**Abstract:** Geothermal water samples taken from deep aquifers within the city of Kaifeng at depths between 800 and 1650 m were analyzed for conventional water chemical compositions and stable isotopes. These results were then combined with the deuterium excess parameter (*d* value), and the contribution ratios of different carbon sources were calculated along with distributional characteristics and data on the migration and transformation of geothermal water. These results included the conventional water chemical group, hydrogen, and oxygen isotopes ( $\delta D$ - $\delta^{18}O$ ), dissolved inorganic carbon (DIC) and associated isotopes ( $\delta^{13}C_{DIC}$ ). The results of this study show that geothermal water in the city of Kaifeng is weakly alkaline, water chemistry mostly comprises a  $HCO_3$ -Na type, and the range of variation of  $\delta D$  is between  $-76.12\text{‰}$  and  $-70.48\text{‰}$ , (average:  $-74.25\text{‰}$ ), while the range of variation of  $\delta^{18}O$  is between  $-11.08\text{‰}$  and  $-9.41\text{‰}$  (average:  $-10.15\text{‰}$ ). Data show that values of *d* vary between  $1.3\text{‰}$  and  $13.3\text{‰}$  (average:  $6.91\text{‰}$ ), while DIC content is between 91.523 and 156.969 mg/L (average: 127.158 mg/L). The recorded range of  $\delta^{13}C_{DIC}$  was between  $-10.160\text{‰}$  and  $-6.386\text{‰}$  (average:  $-9.019\text{‰}$ ). The results presented in this study show that as depth increases, so do  $\delta D$  and  $\delta^{18}O$ , while *d* values decrease and DIC content and  $\delta^{13}C_{DIC}$  gradually increase. Thus,  $\delta D$ ,  $\delta^{18}O$ , *d* values, DIC, and  $\delta^{13}C_{DIC}$  can all be used as proxies for the burial characteristics of geothermal water. Because data show that the changes in *d* values and DIC content are larger along the direction of geothermal water flow, so these proxies can be used to indicate migration. This study also shows demonstrates that the main source of DIC in geothermal water is  $CO_2$  that has a biological origin in soils, as well as the dissolution of carbonate minerals in surrounding rocks. Thus, as depth increases, the contribution of soil biogenic carbon sources to DIC decreases while the influence of carbonate dissolution on DIC increases.

**Keywords:** carbon isotopes; deuterium excess parameter; geothermal water; hydrogen and oxygen isotopes; inorganic carbon; retention time

## 1. Introduction

Stable isotope compositions can be used to measure the biogeochemical behavior of groundwater, including determining sources and recharge [1–5], the evolution of water quality [6], and transitions between surface and groundwater [7,8]. Geothermal water is abundant deep underground around the city of Kaifeng, Henan Province, China, and contains a variety of minerals that are beneficial to

humans [9], so it can be used for drinking, bathing, medical treatment, and health care. However, the scale and intensity of geothermal water resources utilization has gradually expanded, leading to a series of environmental and geological problems [10–12], including a decrease in water volume, a deterioration in quality, and reduced water temperature. With the acceleration of urban construction and the continuous improvement of living standards, the demand for geothermal water is also increasing. As a result, it has become critically important to study the evolutionary process of geothermal water in this region, which is helpful for solving the contradiction between geothermal water development and protection, and providing an important reference for the development and utilization of geothermal water in Henan province, and even in the North China Plain.

Hydrogen and oxygen isotopes in water (i.e.,  $\delta D$ - $\delta^{18}O$ ), often referred to as “fingerprints” [13,14], can be used to extract information about the water cycle, including the sources [15], migration [16], retention, and excretion of the groundwater [17,18]. After entering an underground aquifer, precipitation of atmospheric water will react with the rock, leading to isotope exchange between the two. However, because of the low content of hydrogen in underground rocks, isotope exchange mainly comprises oxygen. The deuterium excess parameter, or  $d$  value ( $d = \delta D - 8\delta^{18}O$ ) [19,20], is often used to study groundwater, because it gives an indication of the degree of water rock oxygen isotope exchange [21], as well as variation within a certain area [22]. Since the main factors restricting groundwater remain essentially the same, the  $d$  value for one aquifer will vary according to length of groundwater residence time; a change from high to low can thus indicate the direction of groundwater flow.

The global carbon cycle has attracted widespread attention, especially in the case of the hydrosphere [23]. Dissolved inorganic carbon (DIC) as well as changes in carbon isotopes in water can reveal geochemical behavior and biogeochemical cycling. Indeed, DIC in groundwater, as well as its isotopic composition ( $\delta^{13}C_{DIC}$ ), are mainly influenced by migration and the environment of occurrence [24,25]. Thus,  $\delta^{13}C_{DIC}$  can be used as a tracer for the evolution of groundwater carbonate in order to understand characteristics of the biogeochemical carbon cycle and to reveal underlying controls on groundwater quality.

In this study, we analyze burial distribution characteristics of conventional water chemical components,  $\delta D$ ,  $\delta^{18}O$ ,  $\delta^{13}C_{DIC}$ ,  $d$  value, and DIC, in different geothermal water depths in the city of Kaifeng. This analysis enables us to reveal characteristics of geothermal water runoff and excretion, determine the mechanisms of water-rock interactions, and lay the scientific foundations for protection and the sustainable utilization of geothermal water resources.

## 2. Materials and Methods

### 2.1. Hydrogeological Characteristics

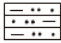
The city of Kaifeng, Henan Province, China, is located in the center of the east Henan plain, in the southeastern corner of the Jiyuan-Kaifeng tectonic sag. Cenozoic strata around this city are loose, porous, and have a thickness between 3000 and 3500 m; these rocks are composed of silty, fine, medium, and coarse sand units which can be divided into Paleogene, Neogene (N), and Quaternary ages. Amongst these, Paleogene strata comprise the basement of the geothermal aquifer within the city, while Quaternary strata are the most recent sedimentary cover within the study area. Thus, the Neogene strata between this basement and cover are divided into the Guantao (Ng) and Minghuazhen (Nm) formations and contain lots of geothermal water. The deep geothermal water in this paper therefore denotes underground hot water at depths between 800 and 1650 m. This resource is located within the Nm and Ng aquifer and mainly comprises fine, medium-fine, and fine silty sand, marl, and other loose sediments. The thickness of this aquifer accounts for between 18% and 68% of the total thickness of strata within this area, and has a porosity between 20% and 28%. It is known from geological drilling data that groundwater within this region flows from southwest to northeast under natural conditions. Since 1997, we have carried out a number of

experiments on hydrochemical monitoring, water level observation, and pumping-reinjection test of geothermal wells in Kaifeng. Monitoring data show that the present groundwater table occurs at depths between 60 and 80 m, and that the geothermal gradient is between 3.20 and 3.60 °C/(100 m) (average: 3.39 °C/(100 m)) [26]. Test data [10,27] from pumping show that the water inflow per unit of aquifer is between 1.55 and 3.48 m<sup>3</sup>/(h·m), the coefficient of transmissibility is between 58.38 and 113.80 m<sup>2</sup>/day, the permeability coefficient is between 0.525 and 1.290 m/day, and the coefficient of storage is between 0.00016 and 0.00065. Thus, when depth is less than 1200 m, the total dissolved solids (TDS) in geothermal water are less than 1 g/L, but when the depth is greater than 1200 m, TDS are greater than 1 g/L. The hydrochemical classification of this geothermal water is HCO<sub>3</sub>-Na type.

## 2.2. Sample Collection and Testing

According to burial conditions, hydraulic characteristics, and the exploitation of geothermal water within the city of Kaifeng, we collected and analyzed 18 samples from different geothermal wells at depths between 800 and 1650 m. Sampling was carried out in March 2015; when collecting geothermal water, the outlet nearest to each geothermal well was selected and drained continuously; geothermal water was sampled after temperature was stabilized in polypropylene bottles that had been cleaned with 10% HCl and thoroughly rinsed with deionized water prior to use. Samples for hydrogen and oxygen isotope analysis were filtered by syringe (20 mL) with filter (cellulose acetate material, pore size 0.22 µm) and sealed in 3 mL brown plastic bottles after ensuring no bubbles were in the bottle. Samples for the analysis of dissolved inorganic carbon isotopes were filtered and then sealed with 2 drops of saturated mercuric chloride solution. Some measurements were performed on-the-spot, including temperature, pH, electrical conductivity, and total dissolved solids (Table 1), and the isotope samples were sent to the experimental test center of the Geological Environmental Monitoring Institute in Henan Province for full water quality analysis (Table 1) within 24 h of collection. Hydrogen and oxygen isotope concentrations in water samples were tested in the Key Laboratory of Henan Polytechnic University (Jiaozuo, China), and we used a pyrolysis method to reduce hydrogen and oxygen in samples to H<sub>2</sub> and CO under high temperature. These gases were then separated onto a chromatographic column with helium carrier gas and introduced into an isotope ratio mass spectrometer (IRMS) (Thermo Scientific MAT 253, Karlsruhe, Germany) ion source to achieve the simultaneous determination of δD and δ<sup>18</sup>O. In this experiment, GBW04458 (δ<sup>18</sup>O = −0.15 ± 0.07, δD = −1.7 ± 0.4), GBW04459 (δ<sup>18</sup>O = −8.61 ± 0.08, δD = −63.4 ± 0.6), and GBW04460 (δ<sup>18</sup>O = −19.13 ± 0.07, δD = 144.0 ± 0.8) were used as standards to calibrate the reference gas, as well as to correct experimental results. Our test precision for δD and δ<sup>18</sup>O were 2‰ and 0.2‰, respectively, while pre-treated water samples were burned in an oxygen-fuel reactor at 1020 °C, and CO<sub>2</sub> that was generated was introduced into the IRMS with the helium carrier gas, so as to realize the determination of the inorganic carbon isotopes. In all cases, δ<sup>13</sup>C<sub>DIC</sub> values were calculated using V-PDB (Vienna Pee Dee Belemnite) as the standard, and the test precision for δ<sup>13</sup>C<sub>DIC</sub> reached 0.2‰.

**Table 1.** Chemical composition and stable isotopic composition of geothermal water in Kaifeng city.

Geothermal Well	Depth (m)	Stratum 	Temperature (°C)	pH	Na <sup>+</sup> (mg/L)	K <sup>+</sup> (mg/L)	Ca <sup>2+</sup> (mg/L)	Mg <sup>2+</sup> (mg/L)	Cl <sup>−</sup> (mg/L)	SO <sub>4</sub> <sup>2−</sup> (mg/L)	HCO <sub>3</sub> <sup>−</sup> (mg/L)	NO <sub>3</sub> <sup>−</sup> (mg/L)	H <sub>2</sub> SiO <sub>3</sub> (mg/L)	DIC (mg C/L)	δ <sup>13</sup> C <sub>DIC</sub> (‰)	δD (‰)	δ <sup>18</sup> O (‰)	d (‰)
W1	950	Nm	48	8.22	209.80	2.93	4.81	1.46	29.42	28.34	493.65	5.04	28.6	102.45	−9.79	−75.28	−11.08	13.30
W2	1000	Nm	40	8.18	199.70	2.18	4.81	2.92	34.39	28.34	454.60	1.09	27.3	91.52	−10.16	−74.16	−9.98	5.70
W3	1001	Nm	48	8.19	199.00	2.81	4.81	2.92	29.42	28.34	479.62	4.53	27.3	105.41	−9.99	−75.12	−10.41	8.20
W4	1139	Nm	57	7.58	302.20	4.59	4.81	2.92	41.12	90.78	663.90	0.22	29.9	145.27	−8.78	−75.30	−10.05	5.10
W5	1200	Nm	50.5	8.04	236.40	3.35	4.81	2.92	34.39	45.63	560.77	1.17	28.6	138.30	−9.65	−75.30	−10.18	6.10
W6	1200	Nm	52	8.12	219.00	3.31	4.81	2.92	29.42	34.10	546.74	1.40	23.4	135.86	−9.48	−74.29	−10.65	10.90
W7	1200	Nm	54	7.91	226.40	4.29	11.82	8.63	44.67	73.97	524.77	2.02	26.0	123.12	−9.44	−72.18	−10.15	9.00
W8	1200	Nm	55	8.08	254.30	3.68	4.81	2.92	32.61	51.39	596.78	<0.01	32.5	121.99	−9.64	−73.49	−9.84	5.20
W9	1202	Nm	51	8.18	229.80	3.54	4.81	2.92	29.42	45.63	549.79	0.88	28.6	117.31	−9.42	−74.33	−9.96	5.30
W10	1205	Ng	52.5	8.21	224.20	2.91	4.81	2.92	29.42	45.63	524.77	<0.01	31.2	135.77	−9.98	−74.29	−10.84	12.40
W11	1250	Ng	53	8.19	184.00	2.32	4.81	2.92	36.16	51.39	418.60	0.38	19.5	124.40	−9.64	−72.22	−10.27	9.90
W12	1251	Nm	53	8.18	274.20	3.85	4.81	2.92	30.84	62.44	619.35	0.15	31.2	126.29	−9.15	−76.12	−10.76	9.98
W13	1254	Nm	53.5	8.10	272.60	4.10	4.81	2.92	36.16	85.49	610.81	0.09	31.2	156.97	−8.81	−74.57	−9.77	3.60
W14	1350	Ng	50	9.33	247.70	5.03	4.81	2.92	41.12	102.30	404.56	12.44	20.8	124.15	−7.85	−70.48	−9.93	8.90
W15	1350	Ng	66	7.92	573.80	12.46	19.04	8.63	60.23	119.59	538.20	0.40	37.7	146.56	−6.39	−75.89	−9.82	2.66
W16	1370	Ng	57	8.11	270.00	4.34	4.81	2.92	32.61	68.20	624.84	0.21	28.6	134.48	−9.09	−74.63	−9.89	4.40
W17	1600	Ng	64	7.90	282.50	4.50	4.81	2.92	32.61	85.49	644.37	0.15	29.9	140.24	−8.65	−74.92	−9.67	2.50
W18	1638	Ng	65	7.43	300.50	5.21	4.81	2.92	34.39	102.30	680.98	0.09	35.1	118.78	−6.43	−73.99	−9.41	1.30

### 3. Results and Discussion

#### 3.1. The Chemical Characteristics of Water

It is clear that pH values of geothermal water from deep pore reservoirs in the city of Kaifeng range between 7.43 and 9.33 (average: 8.10) (Table 1). This geothermal water is weakly alkaline; because it has a total hardness ( $\text{CaCO}_3$  content) that is less than 100 mg/L, it is considered soft water. The cations in this water include  $\text{Na}^+$ ,  $\text{Ca}^{2+}$ ,  $\text{Mg}^{2+}$ , and  $\text{K}^+$ ; of these,  $\text{Na}^+$  content is highest, between 184.0 and 573.8 mg/L (average: 261.45 mg/L). In contrast, contents of  $\text{Ca}^{2+}$ ,  $\text{Mg}^{2+}$ , and  $\text{K}^+$  are generally lower, while the concentration of  $\text{Ca}^{2+}$  ranges between 4.81 and 19.04 mg/L (average: 5.99 mg/L), the concentration of  $\text{Mg}^{2+}$  ranges between 1.46 and 8.63 mg/L (average: 3.47 mg/L), and the concentration of  $\text{K}^+$  ranges between 2.18 and 12.46 mg/L (average: 4.19 mg/L). In contrast, anions in city of Kaifeng geothermal water include  $\text{HCO}_3^-$ ,  $\text{Cl}^-$ ,  $\text{SO}_4^{2-}$ , and  $\text{NO}_3^-$ . Of these, the average concentration is  $\text{HCO}_3^- > \text{Cl}^- > \text{SO}_4^{2-} > \text{NO}_3^-$ .

The hydrochemistry type of the W15 geothermal well is Cl-Na, while that of the others is  $\text{HCO}_3$ -Na. The content of  $\text{H}_2\text{SiO}_3$  in geothermal water is higher, most of them are above 25 mg/L, and the highest content can reach 35.1 mg/L. Hydrochemical components of geothermal water across the study area are not very different horizontally but increase in the vertical direction as burial depth increases. This is mainly because of greater depth, higher temperature, and because the reaction between geothermal water and surrounding rock is more intense; the more chemicals dissolve, the more complex are the water components. In addition, as depth increases, rock formation becomes denser, water circulation conditions become worse, and the retention of geothermal water in surrounding rock increases, which also leads to increases in other hydrochemical components.

#### 3.2. Isotope Characteristics of $\delta\text{D}$ - $\delta^{18}\text{O}$

Previous research [28,29] has shown that the main geothermal water supply source within the city of Kaifeng is precipitation from the southwestern mountainous area of Zhengzhou. This is corroborated by the fact that the equation for atmospheric precipitation in the mountains of southwest Zhengzhou is  $\delta\text{D} = 8.013\delta^{18}\text{O} + 8.275$  [30]. Thus, the following analysis is based on this precipitation equation as well as the atmospheric precipitation equation for Henan (i.e.,  $\delta\text{D} = 6.5019\delta^{18}\text{O} - 3.5793$ ) [31]. As seen Figure 1, hydrogen and oxygen isotopes of geothermal water in Kaifeng are distributed in the vicinity of the atmosphere precipitation line in the southwestern mountains area of Zhengzhou and deviate from the atmosphere precipitation line for Henan. This further corroborates the fact that geothermal water in this region derives from precipitation in the southwestern mountains area of Zhengzhou. On the basis of data presented in Table 1,  $\delta\text{D}$  varies from  $-76.12\text{‰}$  to  $-70.48\text{‰}$ , with an average value of  $-74.25\text{‰}$ , while  $\delta^{18}\text{O}$  varies from  $-11.08\text{‰}$  to  $-9.41\text{‰}$ , with an average value of  $-10.15\text{‰}$ . The content of  $\delta^{18}\text{O}$  in oxidiferous minerals, including carbonates and silicates, is much higher than in geothermal water, so there is isotopic exchange between geothermal water and oxidiferous minerals, resulting in an increase of  $\delta^{18}\text{O}$  in geothermal water. This process is called “oxygen drift”.

The changes of  $\delta\text{D}$  and  $\delta^{18}\text{O}$  in geothermal water reported in this study can be seen in Figure 2, which increases with the increase in depth, and have amplitude of variation of 7.41% and 15.07%, respectively; these results show that the groundwater within the thermal reservoir had a longer circulation time, and that there is obvious water-rock interaction. Because of the low content of hydrogen in rock-forming minerals, however, the isotopic exchange intensity of  $\delta\text{D}$  is lower than  $\delta^{18}\text{O}$ , which leads to a difference in their growth rate. This means that  $\delta^{18}\text{O}$  has higher enrichment in geothermal water than  $\delta\text{D}$  when water-rock interaction occurs. Therefore, with the increase of the depth and temperature, the effect of water-rock interaction on enrichment of  $\delta^{18}\text{O}$  is larger than  $\delta\text{D}$ , and the enrichment of  $\delta^{18}\text{O}$  is more obvious with increasing depth, which is mainly the result of the higher temperature of deep geothermal water. This accelerates the water-rock interaction rate.

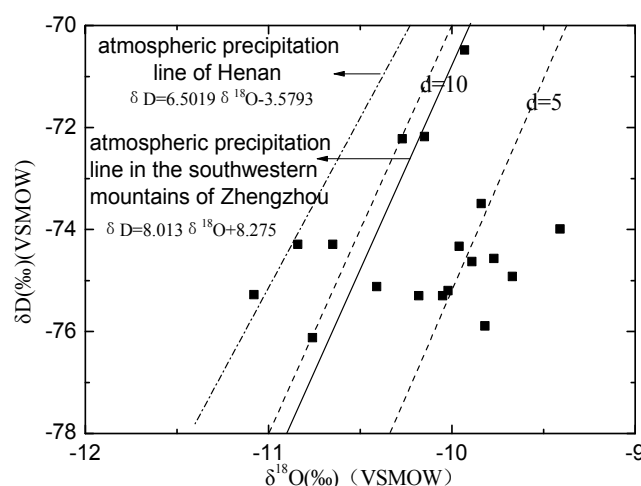


**Figure 1.** Relationship between  $\delta D$  and  $\delta^{18}O$  and the characteristic of the  $d$  value in Kaifeng geothermal water.

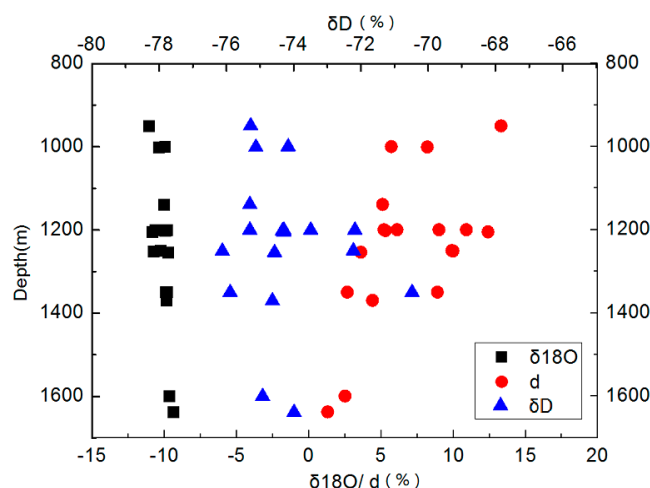


**Figure 2.** Variations of  $\delta D$ ,  $\delta^{18}O$ , and  $d$  value of deep geothermal water with depths in Kaifeng.

Because of more geothermal water samples from geothermal wells at depths of about 1200 m, spatial distribution characteristics of  $\delta D$  and  $\delta^{18}O$  in geothermal water at this depth can be analyzed. The data presented in Table 1 show that there are five geothermal wells in this region that have depths of about 1200 m; these all belong to the Neogene Nm unit and include W5, W6, W7, W8, and W9 (Figure 1), as well as, W6, W7, and W9 in the southwest of the study area. In the latter three of these wells,  $\delta D$  and  $\delta^{18}O$  have average values of  $-73.60\text{‰}$  and  $-10.25\text{‰}$ , respectively, while in wells W5 and W8, located in the northeast of the study area, average values were  $-74.40\text{‰}$  and  $-10.01\text{‰}$ , respectively. These results show that the  $\delta D$  of geothermal water reduces slightly from the southwest to the northeast, while the  $\delta^{18}O$  of geothermal water increases slightly.

### 3.3. $D$ Value Characteristics

The magnitude  $d$  values are not only related to the retention time of geothermal water in an aquifer, but also depend on the depth of the formation and the chemical composition of the oxygen compounds in the rock [32,33]. There are several reasons for this, including differences in depth, densities of rock strata, conditions of water circulation, and different structural types and chemical compositions of minerals, leading to different solubility in water-rock interactions. These factors ultimately make the capacity of water-rock oxygen isotope exchange different.



D values for geothermal water within Kaifeng range between 1.3‰ and 13.3‰ (see Table 1), with an average of 6.91‰. As we can see from Figure 2, in general, d values gradually decrease with the increase of depth. However, in order to reveal changes in d values vertically, six geothermal wells, including W1, W3, W6, W9, W15, and W17, in the south of the study area and close to each other, were analyzed. The average d value of geothermal water 1000 m below the surface is 10.75‰, while the average d value for geothermal water 1200 m below the surface is 8.10‰, and the average d value for geothermal water 1400 m below the surface is 2.66‰ (Table 1). The average d value for geothermal water 1600 m below the surface is 2.50‰. These results also illustrate the fact that d values decrease as burial depth increases, because the deeper the burial depth, the denser the rock strata, the worse the conditions of water circulation, the more complete the interaction between geothermal water and the surrounding rock, and the greater the oxygen drift. All these factors result in smaller d values.

Within the same strata, because similar factors influence water-rock isotopic exchange, the d values of geothermal water may be related to residence time in an aquifer. In other words, along the direction of geothermal water runoff, residence time in a thermal reservoir will be longer and interaction of geothermal water with surrounding rock will increase. This leads to a gradually reducing d value. Thus, we take geothermal water from the Nm unit at a depth of 1200 m as an example to analyze variation of d values horizontally to describe the migration of geothermal water. In this example, W6, W7, and W9 are three geothermal wells located in the southwestern part of the study area; the average d value in this geothermal water is 8.40‰, while W5 and W8, two geothermal wells located in the northeastern part of the study area, have an average d value of 5.65‰. Results show that the d value gradually reduces from the southwest to the northeast horizontally, which shows that the residence time of geothermal water in thermal reservoirs gradually increases from southwest to the northeast. This indicates that the direction of geothermal water flow is southwest-to-northeast; indeed, residence time of geothermal water in the thermal reservoir is longer in this direction, and isotopic exchange of carbonate is more obvious, leading to a gradually reduced d value.

### 3.4. DIC and $\delta^{13}\text{C}_{\text{DIC}}$ Characteristics

There are three main forms of DIC in groundwater:  $\text{HCO}_3^-$ , dissolved  $\text{CO}_2$ , and  $\text{CO}_3^{2-}$ . On the basis of the data presented, the geothermal water in Kaifeng is weakly alkaline, and the hydrochemical type is  $\text{HCO}_3\text{-Na}$  [9]; therefore, the main form of DIC in geothermal water is  $\text{HCO}_3^-$ . Test results show that the content of DIC in deep geothermal water was between 91.52 and 156.97 mg/L (average: 127.16 mg/L), while  $\delta^{13}\text{C}_{\text{DIC}}$  ranged between  $-10.16\text{‰}$  and  $-6.39\text{‰}$  (average:  $-9.02\text{‰}$ ).

The distributions of DIC and  $\delta^{13}\text{C}_{\text{DIC}}$  in the vertical direction are shown in Figure 3. These data show that DIC and  $\delta^{13}\text{C}_{\text{DIC}}$  increase with depth; indeed, from the previous analysis we can know that, in the vertical direction, as depth increases, the temperature of the thermal reservoir increases, and the speed of water-rock reaction is accelerated, which leads to the increase of DIC and  $\delta^{13}\text{C}_{\text{DIC}}$ . The difference, however, is in growth rate; as depth increases, the growth rate of DIC gradually becomes smaller, while the growth rate of  $\delta^{13}\text{C}_{\text{DIC}}$  gradually increases. These results indicate that the source of DIC in geothermal water may change with increasing of depth, so it can be inferred that the sources of DIC in geothermal water at different depths in Kaifeng city are different.

Spatial variations of DIC and of deep geothermal water in Kaifeng are shown in Figure 4. Changes in DIC and  $\delta^{13}\text{C}_{\text{DIC}}$  in the horizontal direction were also analyzed using geothermal water from the Nm Formation from a depth of about 1200 m. The average values of DIC and  $\delta^{13}\text{C}_{\text{DIC}}$  of W6, W7, and W9 in the southwestern part of the study area were 125.43 mg/L and  $-9.45\text{‰}$ , while average values of DIC and  $\delta^{13}\text{C}_{\text{DIC}}$  of W5 and W8 in the northeast were 130.15 mg/L and  $-9.64\text{‰}$ , respectively. These data show that DIC contents increases and  $\delta^{13}\text{C}_{\text{DIC}}$  decreases slightly along the direction of groundwater flow because the dissolution of carbonates requires participation of  $\text{CO}_2$  from a biological soil origin, although longer residence time can increase the dissolution of carbonate; accordingly, the proportion of  $\text{CO}_2$  involved in this reaction also gradually increases, leading to a slightly negative deviation in  $\delta^{13}\text{C}_{\text{DIC}}$ .

Thus, in the horizontal direction, variety of  $\delta^{13}\text{C}_{\text{DIC}}$  was less affected by the residence time of geothermal water, while the content of DIC was greatly influenced by, and increased as a result of, residence time.

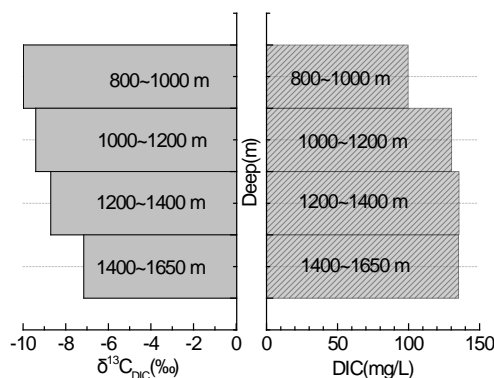


**Figure 3.** Dissolved inorganic carbon (DIC) and  $\delta^{13}\text{C}_{\text{DIC}}$  of geothermal water at different burial depths.

In sum,  $\delta\text{D}$ ,  $\delta^{18}\text{O}$ , d value, DIC, and  $\delta^{13}\text{C}_{\text{DIC}}$  all exhibit regular changes with increasing depth in the vertical direction. These changes include  $\delta\text{D}$  and  $\delta^{18}\text{O}$  increasing gradually, d value decreasing, and DIC and  $\delta^{13}\text{C}_{\text{DIC}}$  increasing gradually. Thus,  $\delta\text{D}$ ,  $\delta^{18}\text{O}$ , d value, DIC, and  $\delta^{13}\text{C}_{\text{DIC}}$  can be used to indicate the burial characteristics of geothermal water in the city of Kaifeng. In the horizontal direction, variation in  $\delta\text{D}$ ,  $\delta^{18}\text{O}$ , and  $\delta^{13}\text{C}_{\text{DIC}}$  are relatively slight, while variation in d values and DIC are relatively large along the direction of geothermal water flow. Thus, d values and DIC can be used to indicate the migration of geothermal water in the city of Kaifeng.

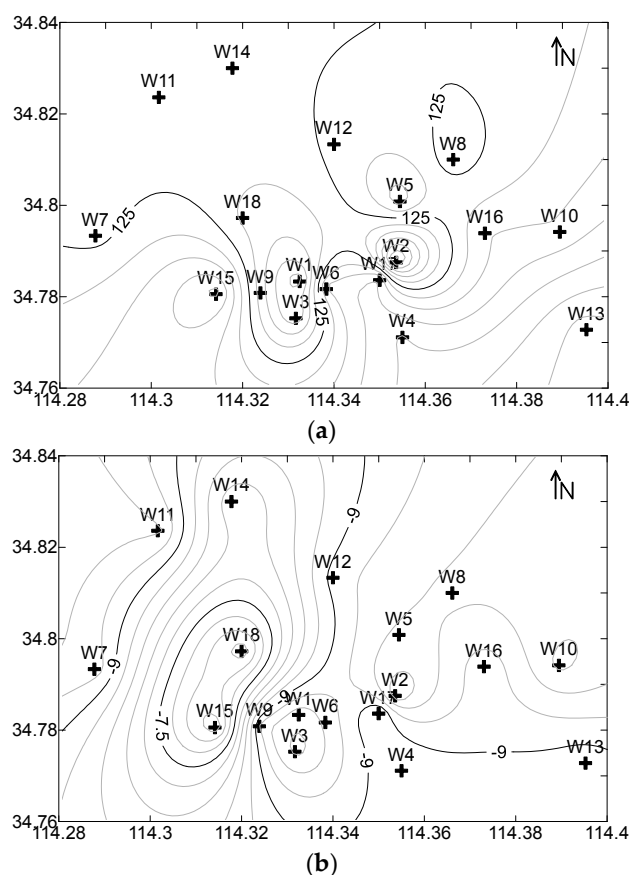


**Figure 4.** Spatial variations of DIC (a) and  $\delta^{13}\text{C}_{\text{DIC}}$  (b) of deep geothermal water in Kaifeng.



#### 4. Composition of DIC Sources

Studies have shown that the carbon isotope composition of different sources are obviously different. For example, the  $\delta^{13}\text{C}$  of carbonate minerals is usually between  $-3\text{‰}$  and  $2\text{‰}$  [34,35], while the  $\delta^{13}\text{C}$  of atmospheric  $\text{CO}_2$  is usually about  $-7\text{‰}$  [36,37], and the  $\delta^{13}\text{C}$  of  $\text{CO}_2$  from the mantle is usually between  $-11\text{‰}$  and  $-4\text{‰}$  [23]. At the same time, the  $\delta^{13}\text{C}$  of  $\text{CO}_2$  produced by soil organisms (i.e., the root respiration of plants, microbial activity, and the degradation of organic matter) varies greatly, usually by  $-25\text{‰}$  in humid climatic regions and  $-12\text{‰}$  in arid climatic region [38]. Thus,  $\delta^{13}\text{C}_{\text{DIC}}$  can be used to indicate sources of DIC. For deep geothermal water in the city of Kaifeng, a medium-to-low temperature geothermal resource, the carbon source from the mantle  $\text{CO}_2$ , is very limited, and the carbon source from atmospheric  $\text{CO}_2$  is also very weak. This latter source can effectively be neglected. In addition, we also calculated the saturated index of calcium carbonate in geothermal water and found that the saturation index of calcium carbonate is basically negative, indicating that calcium carbonate has not yet reached full saturation; therefore, calcium carbonate is mainly dissolved rather than precipitated. Thus, building on the hydrogen and oxygen isotope analysis in the previous section, it is clear that the residence time of geothermal water is relatively long, so the source of DIC may be the reaction of  $\text{CO}_2$  and carbonate minerals in surrounding rock. Thus,  $\text{CO}_2$  is therefore derived mainly from soil biological action and then dissolved in geothermal water.

In order to estimate the contribution ratio of the two carbon sources to DIC,  $\text{CO}_2$  from soil biological action, and carbonate minerals in surrounding rock, the following binary mixing model [39] was used to calculate the source of DIC:

$$\delta^{13}\text{C}_{\text{DIC}} = \left[ \sum_0^i (mC_i) (\delta^{13}\text{C}_i) \right] / \left[ \sum_0^i (mC_i) \right] \quad (1)$$

In this expression,  $\delta^{13}\text{C}_{\text{DIC}}$  is the measured value (‰) of inorganic carbon isotopes in geothermal water,  $mC_i$  is the content of inorganic carbon from the  $i$ th carbon source (mg/L), and  $\delta^{13}\text{C}_i$  is  $\delta^{13}\text{C}$  of the  $i$ th carbon source (‰).

We assume that the  $\delta^{13}\text{C}$  of carbonate minerals is  $-0.5\text{‰}$  and the  $\delta^{13}\text{C}$  of soil biogenic  $\text{CO}_2$  is  $-12\text{‰}$ . Thus, on the basis of Equation (1), different sources can be invoked for inorganic carbon in geothermal water at different depths. In the case of geothermal water at depths less than 1300 m in Kaifeng, for example, the proportion of inorganic carbon from carbonate is in the range 16% and 28% (average: 21%), while the proportion of inorganic carbon from soil biogenic  $\text{CO}_2$  is between 72% and 84% (average: 78%). In the case of geothermal water at depths of more than 1300 m, the proportion of inorganic carbon from carbonate is between 25% and 49% (average: 37%), while the proportion of inorganic carbon from soil biogenic  $\text{CO}_2$  is between 51% and 75% (average: 63%).

The above calculation results show that as depth increases, the proportional contribution of carbon source from carbonate dissolution to DIC in the deep geothermal waters of Kaifeng increase, while the contribution to the  $\text{CO}_2$  carbon source produced by soil biological action to DIC decreases. As depth increases, temperature and lithology clearly change, which affects water-rock reactions and the isotopic exchange of inorganic carbon. As a result, both DIC and  $\delta^{13}\text{C}_{\text{DIC}}$  are exchanged in the vertical direction, and variations in temperature and lithology lead to the changes of DIC and  $\delta^{13}\text{C}_{\text{DIC}}$  with depth. That is, as the depth increases, the inorganic carbon isotope gradually deviates to the positive direction, and the DIC content gradually stabilizes. However, the contribution of carbonate dissolved to DIC increased from 21% to 37%, while the contribution of soil biogenic  $\text{CO}_2$  to DIC decreased from 78% to 63%.

#### 5. Conclusions

As the depth of geothermal water in the city of Kaifeng increases, so do the temperatures of thermal reservoirs. At the same time, the speed of water-rock reactions are accelerated, which means that the content of DIC increases;  $\delta\text{D}$ ,  $\delta^{18}\text{O}$ , and  $\delta^{13}\text{C}_{\text{DIC}}$  exhibit different enrichment degrees,

while  $d$  values decrease. Therefore, variation in  $\delta D$ ,  $\delta^{18}O$ ,  $d$  value, DIC, and  $\delta^{13}C_{DIC}$  can be used as proxies for the burial characteristics of geothermal water. Along the direction of geothermal water flow in Kaifeng,  $\delta D$ ,  $\delta^{18}O$ , and  $\delta^{13}C_{DIC}$ , all buried in the Nm Formation to depths of about 1200 m, did not change significantly, while  $d$  value and DIC varied greatly. Thus, it is better to use  $d$  values and DIC as proxies for groundwater migration.

The main sources of DIC in deep geothermal water comprise the  $CO_2$  produced by soil biological action and the dissolution of carbonate minerals from surrounding rocks. The contribution ratio of these two sources of carbon to DIC in deep geothermal water changes with increasing depth; in other words, the contribution of carbon source from carbonate dissolution to DIC increases, while that of soil biogenic carbon to DIC decreases gradually.

**Acknowledgments:** This work was financially supported by the National Natural Science Foundation of China (Grant41672240), Innovaton Scientists and Technicians Troop Construction Projects of Henan Province (Grant CXTD2016053), Henan Province's Technological Innovation Team of Colleges and Universities (Grant 15IRTSTHN027), Fundamental Research Funds for the Universities of Henan Province (NSFRF1611), Scientists and Technicians Projects of Henan Province (Grant 172107000004).

**Author Contributions:** Xinyi Wang and Weifang Qiao conceived and designed the experiments; Weifang Qiao and Jing Chen performed the experiments; Weifang Qiao and Xiaoman Liu analyzed the data; Jing Chen and Fang Yang collected water samples; Weifang Qiao wrote the paper; Xinyi Wang and Xiaoman Liu reviewed and edited the manuscript. All authors read and approved the manuscript.

**Conflicts of Interest:** The authors declare no conflicts of interest.

## References

1. Marques, J.M.; Graça, H.; Eggenkamp, H.G.; Neves, O.; Carreira, P.M.; Matias, M.J.; Mayer, B.; Nunes, D.; Trancoso, V.N. Isotopic and hydrochemical data as indicators of recharge areas, flow paths and water–rock interaction in the caldas da rainha–quinta das janelasthermomineral carbonate rock aquifer (central Portugal). *J. Hydrol.* **2013**, *476*, 302–313. [[CrossRef](#)]
2. Cervi, F.; Borgatti, L.; Dreossi, G.; Marcato, G.; Michelini, M.; Stenni, B. Isotopic features of precipitation and groundwater from the eastern alps of Italy: Results from the MT. Tinisa hydrogeological system. *Environ. Earth Sci.* **2017**, *76*, 410. [[CrossRef](#)]
3. Deiana, M.; Mussi, M.; Ronchetti, F. Discharge and environmental isotope behaviours of adjacent fractured and porous aquifers. *Environ. Earth Sci.* **2017**, *76*, 595. [[CrossRef](#)]
4. Mussi, M.; Nanni, T.; Tazioli, A.; Vivalda, P.M. The MT conero limestone ridge: The contribution of stable isotopes to the identification of the recharge area of aquifers. *Ital. J. Geosci.* **2017**, *136*, 186–197. [[CrossRef](#)]
5. Cervi, F.; Ronchetti, F.; Doveri, M.; Mussi, M.; Marcaccio, M.; Tazioli, A. The use of stable water isotopes from rain gauges network to define the recharge areas of springs: Problems and possible solutions from case studies from the northern Apennines. *Geom. Geoling. Ambient. Min.* **2016**, *149*, 19–26.
6. Peng, T.-R.; Wang, C.-H.; Huang, C.-C.; Fei, L.-Y.; Chen, C.-T.A.; Hwong, J.-L. Stable isotopic characteristic of taiwan's precipitation: A case study of western pacific monsoon region. *Earth Planet. Sci. Lett.* **2010**, *289*, 357–366. [[CrossRef](#)]
7. Schiavo, M.; Hauser, S.; Povinec, P. Stable isotopes of water as a tool to study groundwater–seawater interactions in coastal south-eastern Sicily. *J. Hydrol.* **2009**, *364*, 40–49. [[CrossRef](#)]
8. Dotsika, E.; Lykoudis, S.; Poutoukis, D. Spatial distribution of the isotopic composition of precipitation and spring water in Greece. *Glob. Planet. Chang.* **2010**, *71*, 141–149. [[CrossRef](#)]
9. Wang, X.; Zhao, L.; Liu, X.; Lili, A.; Zhang, Y. Temperature effect on the transport of nitrate and ammonium ions in a loose-pore geothermal reservoir. *J. Geochem. Exp.* **2013**, *124*, 59–66. [[CrossRef](#)]
10. Zhao, L.; Wang, X.; Zhang, Q.; Zhang, Y. Study on the transformation mechanism of nitrate in a loose-pore geothermal reservoir: Experimental results and numerical simulations. *J. Geochem. Exp.* **2014**, *144*, 208–215. [[CrossRef](#)]
11. Huang, S.; Tian, T. Sustainable development of geothermal resource in China and future projects. *World Geotherm. Congr.* **2005**, *4*, 24–29.
12. Haiyan, H. Environmental Impact of Geothermal Development in Henan Province, China. Available online: <http://www.os.is/gogn/unu-gtp-report/UNU-GTP-2003-11.pdf> (accessed on 19 December 2017).

13. Schwertl, M.; Auerswald, K.; Schäufele, R.; Schnyder, H. Carbon and nitrogen stable isotope composition of cattle hair: Ecological fingerprints of production systems? *Agric. Ecosyst. Environ.* **2005**, *109*, 153–165. [\[CrossRef\]](#)
14. Hoefs, J. *Stable Isotope Geochemistry*; Springer: Berlin, Germany, 1997; Volume 201.
15. Craig, H. Isotopic composition and origin of the red sea and salton sea geothermal brines. *Science* **1966**, *154*, 1544–1548. [\[CrossRef\]](#) [\[PubMed\]](#)
16. Li, J.; Liu, J.; Pang, Z.; Wang, X. Characteristics of chemistry and stable isotopes in groundwater of the chaobai river catchment, Beijing. *Proced. Earth Planet. Sci.* **2013**, *7*, 487–490. [\[CrossRef\]](#)
17. West, A.; February, E.; Bowen, G.J. Spatial analysis of hydrogen and oxygen stable isotopes (“isoscapes”) in ground water and tap water across South Africa. *J. Geochem. Exp.* **2014**, *145*, 213–222. [\[CrossRef\]](#)
18. Koh, D.-C.; Ha, K.; Lee, K.-S.; Yoon, Y.-Y.; Ko, K.-S. Flow paths and mixing properties of groundwater using hydrogeochemistry and environmental tracers in the southwestern area of jeju volcanic island. *J. Hydrol.* **2012**, *432*, 61–74. [\[CrossRef\]](#)
19. Masson-Delmotte, V.; Jouzel, J.; Landais, A.; Stievenard, M.; Johnsen, S.J.; White, J.; Werner, M.; Sveinbjornsdottir, A.; Fuhrer, K. Grip deuterium excess reveals rapid and orbital-scale changes in greenland moisture origin. *Science* **2005**, *309*, 118–121. [\[CrossRef\]](#) [\[PubMed\]](#)
20. Vimeux, F.; Masson, V.; Jouzel, J.; Petit, J.; Steig, E.; Stievenard, M.; Vaikmae, R.; White, J. Holocene hydrological cycle changes in the southern hemisphere documented in east antarctic deuterium excess records. *Clim. Dyn.* **2001**, *17*, 503–513. [\[CrossRef\]](#)
21. Uemura, R.; Matsui, Y.; Yoshimura, K.; Motoyama, H.; Yoshida, N. Evidence of deuterium excess in water vapor as an indicator of ocean surface conditions. *J. Geophys. Res. Atmos.* **2008**, *113*. [\[CrossRef\]](#)
22. O’neil, J.; Shaw, S.; Flood, R. Oxygen and hydrogen isotope compositions as indicators of granite genesis in the New England batholith, Australia. *Contrib. Miner. Petrol.* **1977**, *62*, 313–328. [\[CrossRef\]](#)
23. Deines, P. The carbon isotope geochemistry of mantle xenoliths. *Earth Sci. Rev.* **2002**, *58*, 247–278. [\[CrossRef\]](#)
24. Li, F.; Pan, G.; Tang, C.; Zhang, Q.; Yu, J. Recharge source and hydrogeochemical evolution of shallow groundwater in a complex alluvial fan system, southwest of north China plain. *Environ. Geol.* **2008**, *55*, 1109–1122. [\[CrossRef\]](#)
25. Warner, N.R.; Kresse, T.M.; Hays, P.D.; Down, A.; Karr, J.D.; Jackson, R.B.; Vengosh, A. Geochemical and isotopic variations in shallow groundwater in areas of the fayetteville shale development, north-central Arkansas. *Appl. Geochem.* **2013**, *35*, 207–220. [\[CrossRef\]](#)
26. Wang, X.; Li, J.; Lin, X.; Liao, Z. Geothermal field characteristics in the Kaifeng city. *Adv. Water Sci.* **2002**, *13*, 191–196.
27. Zhu, H.L.; Liu, X.M.; Yang, F.; Yang, H.J.; Wang, X.Y. Analysis and study on geothermal reijection test of deep groundwater in Kaifeng. *J. Henan Polytech. Univ. (Nat. Sci.)* **2011**, *30*, 215–219.
28. Lin, X.; Tabouré, A.; Wang, X.; Liao, Z. Use of a hydrogeochemical approach in determining hydraulic connection between porous heat reservoirs in Kaifeng area, Henan, China. *Appl. Geochem.* **2007**, *22*, 276–288. [\[CrossRef\]](#)
29. Dong, W.-H.; Kang, B.; Du, S.-H.; Shi, X.-F. Estimation of shallow groundwater ages and circulation rates in the Henan plain, China: CFC and deuterium excess methods. *Geosci. J.* **2013**, *17*, 479–488. [\[CrossRef\]](#)
30. Wang, X.; Han, P.; Liao, Z.; Lin, X. The geochemical method for studying hydraulic relationships among porous medium reservoirs. *J. Hydraul. Eng.* **2001**, *32*, 75–79.
31. Li, M.; Gao, S.; Li, K. Features of hydrogen and oxygen isotopes of quaternary groundwater in Henan plain and the recharge analysis. *Geotech. Investig. Surv.* **2010**, *38*, 42–47.
32. Vodila, G.; Palcsu, L.; Futo, I.; Szántó, Z. A 9-year record of stable isotope ratios of precipitation in eastern Hungary: Implications on isotope hydrology and regional palaeoclimatology. *J. Hydrol.* **2011**, *400*, 144–153. [\[CrossRef\]](#)
33. Stumpp, C.; Klaus, J.; Stichler, W. Analysis of long-term stable isotopic composition in german precipitation. *J. Hydrol.* **2014**, *517*, 351–361. [\[CrossRef\]](#)
34. Jimenez-Lopez, C.; Caballero, E.; Huertas, F.; Romanek, C. Chemical, mineralogical and isotope behavior, and phase transformation during the precipitation of calcium carbonate minerals from intermediate ionic solution at 25 °C. *Geochim. Cosmochim. Acta* **2001**, *65*, 3219–3231. [\[CrossRef\]](#)

35. Li, S.-L.; Calmels, D.; Han, G.; Gaillardet, J.; Liu, C.-Q. Sulfuric acid as an agent of carbonate weathering constrained by  $\delta^{13}\text{C}_{\text{DIC}}$ : Examples from southwest China. *Earth Planet. Sci. Lett.* **2008**, *270*, 189–199. [[CrossRef](#)]
36. Francey, R.; Allison, C.; Etheridge, D.; Trudinger, C.; Enting, I.; Leuenberger, M.; Langenfelds, R.; Michel, E.; Steele, L. A 1000-year high precision record of  $\delta^{13}\text{C}$  in atmospheric  $\text{CO}_2$ . *Tellus B* **1999**, *51*, 170–193. [[CrossRef](#)]
37. Langenfelds, R.; Francey, R.; Pak, B.; Steele, L.; Lloyd, J.; Trudinger, C.; Allison, C. Interannual growth rate variations of atmospheric  $\text{CO}_2$  and its  $\delta^{13}\text{C}$ ,  $\text{H}_2$ ,  $\text{CH}_4$ , and  $\text{CO}$  between 1992 and 1999 linked to biomass burning. *Glob. Biogeochem. Cycles* **2002**, *16*. [[CrossRef](#)]
38. Kuzyakov, Y.; Domanski, G. Carbon input by plants into the soil. Review. *J. Plant Nutr. Soil Sci.* **2000**, *163*, 421–431. [[CrossRef](#)]
39. Carlson, C.A.; Hansell, D.A.; Nelson, N.B.; Siegel, D.A.; Smethie, W.M.; Khatiwala, S.; Meyers, M.M.; Halewood, E. Dissolved organic carbon export and subsequent remineralization in the mesopelagic and bathypelagic realms of the north atlantic basin. *Deep Sea Res. Part II Top. Stud. Oceanogr.* **2010**, *57*, 1433–1445. [[CrossRef](#)]



© 2017 by the authors. Licensee MDPI, Basel, Switzerland. This article is an open access article distributed under the terms and conditions of the Creative Commons Attribution (CC BY) license (<http://creativecommons.org/licenses/by/4.0/>).